1st International Conference on Structural Integrity, ICONS-2014

Using Excitation Invariance in the Characterization of Defects by Eddy Current Image Constructions

A. Lopes Ribeiro[*], D. Pasadas, H. G. Ramos and T. Rocha

Instituto de Telecomunicações, Instituto Superior Técnico, Universidade de Lisboa
Av. Rovisco Pais, 1049-001 Lisboa, Portugal
[*]*E-mail ID:arturlr@tecnico.ulisboa.pt*

Abstract

In this article the eddy current method is used to characterize defects in conductive non-ferromagnetic plates. A special attention is paid to the presentation of results in the form of images. An inverse problem with Tikhonov regularization is solved to obtain the two-dimensional distribution of currents inside the material under test. With this purpose a uniform field probe is used to guarantee a spatially invariant excitation field for probe scanning translations. The probe contains a magnetic field detector based on high sensitivity giant magneto-resistors which reads the magnetic field component parallel to the excitation and induction currents.

Keywords: Non-destructive testing; Eddy currents; Giant magneto-resistor sensors; Inverse problem; Tikhonov regularization.

Introduction

The non-destructive testing (NDT) and evaluation (NDE) is usually performed by skilled personnel. This work is performed manually or with automated equipment. Whatever method is used (e.g.: eddy currents, ultrasound) the data presentation is very important. In the case of the eddy current method, the visualization of the currents inside the material could help the person in charge to accomplish the work.

In this article we shall consider the characterization of defects inside conductive non-ferromagnetic materials using eddy currents and imaging methods. The surface of the material under test shall be scanned, covering a given area, the probe following a prescribed trajectory through a set of step translations.

The choice of the excitation coil must be coherent with the imaging purpose, as well as the excitation type (sinusoidal, pulsed,...). Another important aspect is related to the type of detection of the field disturbances originated by the presence of defects. Having decided on this, we have a signal that has to be processed: amplified, filtered, acquired and finally assembled to form a matrix that represents the image of the measured disturbances. At this time, and before any further image processing, we must take into account the signal to noise ratio of the acquired image in relation to the signal purity of the primary excitation and detection processes. Finally we have got a two dimensional picture describing one physical parameter, say one component of the magnetic field perturbation. In some cases this visual description is considered sufficient and the process ends at this point. However the main goal is the depiction of the material discontinuities themselves.

1.1 Solving the Inverse Problem

The solution of the so-called inverse problem becomes the main issue. This problem is formally described in the following way: starting from the parameter perturbation image determine the spatial distribution of the metal material conductivity. As the problem is ill-posed some a priori information must be introduced into the solution algorithm, e.g., the material is homogeneous almost everywhere, with a constant electric conductivity, but a linear surface crack normal to the surface may be present.

Usually this problem is tackled in two different ways. In the first method the physical problem, which, for the example above could be the determination of the field perturbation due to the presence of a surface crack is solved. Then, this analytical or numerical solution is compared to the experimental data, and the crack parameters are changed in a iterative process, trying to match the model solution with the actual acquired data.
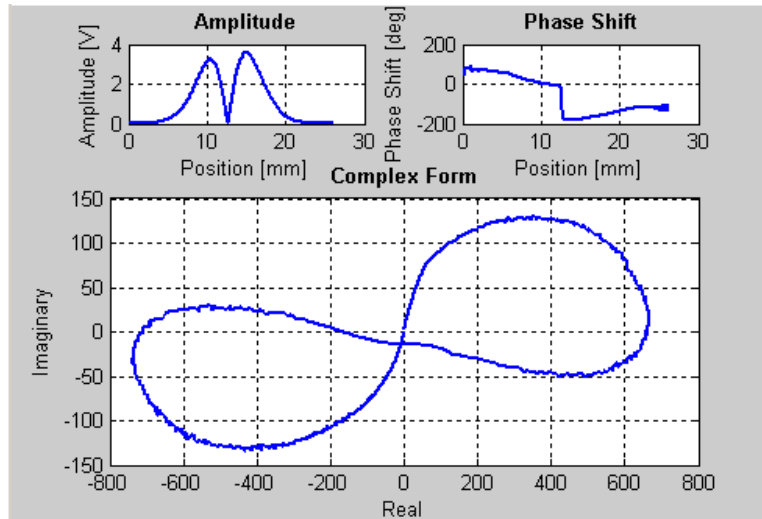

Figure 1. Typical aluminium crack signature obtained with a GMR-EC probe.

In this article our method follows a different path. We shall be concerned on the determination of the eddy current density inside the metal, and the presence of conductivity discontinuities must be inferred from the possible

local vanishing of the eddy current. If we choose a constant field excitation coil, which produces a primary field spatially constant inside a limited area, the primary excitation field is invariant under a probe translation. Thus, the produced eddy currents inside a homogeneous material shall be uniform as well. The magnetic sensing element in our probe must measure the field perturbation originated precisely by the eddy currents perturbation. The perturbation component, being purely inductive, may be represented as a collection of current dipoles. The magnetic field produced by an elemental current dipole may be taken as a transformation kernel, in order to determine the current dipolar density.

The characterization of defects in non-destructive evaluation (NDE) benefits from image representations. Commercial equipment used in manual inspection eddy current methods presents an output curve on a display, usually referred as a signature. This curve is correlated to the nature of the defect. Figure 1 presents one of those signatures obtained with non-commercial self-constructed equipment[1]. Comparison between different signatures obtained by inspection of standard defects permits to train personnel to distinguish between material flaws. The construction of these images, as represented in Fig.1 was obtained when a giant magneto-resistoreddy-current probe (GMR-EC) was moved with constant speed over a defect (e.g.: an aluminium crack). The image representation is obviously an improvement over any other form of signal representation. Thus, it is quite natural to put the following question:

Isn't it possible to obtain an image with the geometrical representation of the flaws?

In the following sections this article is outlined as follows: In section two the current coil to produce a spatially invariant excitation is described. The nature of the induction currents when in presence of a defect is described as well. Section three describes the equipment in use to construct a map of a single field component. Section four presents some modelling results describing the current geometry around a linear crack and how these results may be interpreted as the solution of the direct problem. Section five describes the Tikhonov regularization used in the inverse problem solution and section six shows some regularized results of the current distribution around a linear crack.

2. The Excitation Current Coil

2.1 Using a Pancake Coil

A two-dimensional image may be constructed when we scan a given area where a defect is enclosed.If a pancake coil is used to excite eddy currents inside a non-ferromagnetic conductor,the non-homogeneity of the conductor material or the existence of any discontinuities causes a deformation of the currents that may be translated into the modification of the secondary magnetic field produced by the eddy currents. The two-dimensional representation of any parameter of this field (e.g.: amplitude or phase under sinusoidal excitation) or the representation of the excitation coil impedance (modulus or angle) shows the location of the defects but is not directly representative of the defect geometry. Some advantage may be taken from the fact that the pancake probe excitation field is invariant under rotations. However, if a single-axis GMR sensor is used to measure one component of the field parallel to the metal surface quite different images are obtained depending on the GMR sensor axis orientation. Figure 2 represents those direct images. Being quite different from each other, it is difficult to characterize a defect by inspection of such image, The best thing to do is to obtain several pictures at different angles and choose the best representation for a defect. These pictures may be obtained by software composition from those depicted in Fig.2 which were obtained at orthogonal angles [2].
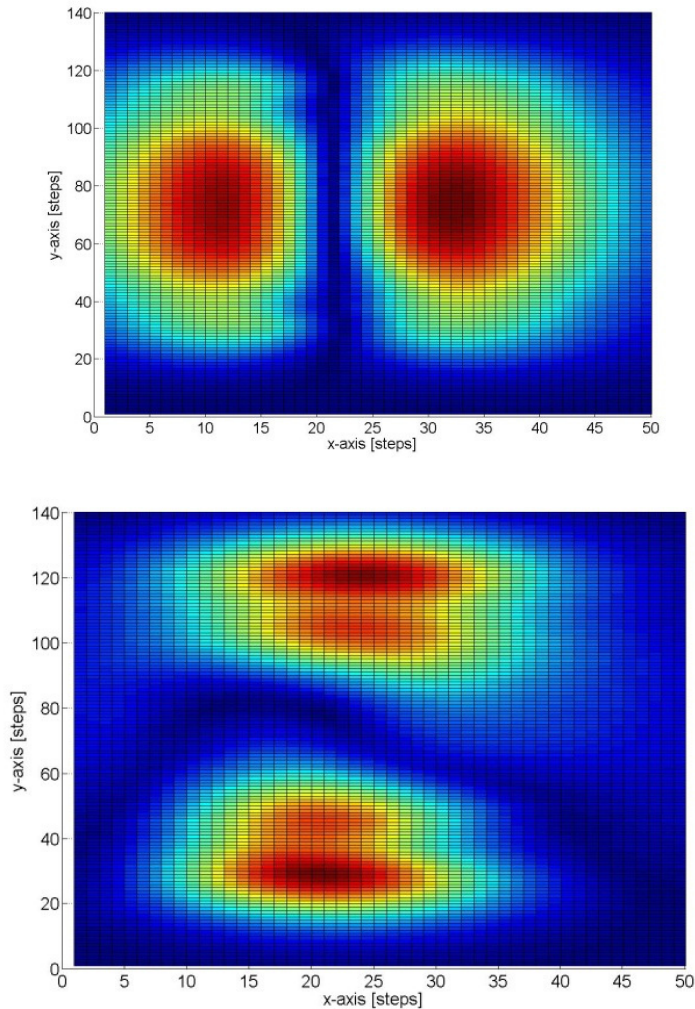
Figure 2. Two images from the same crack obtained with orthogonal angles of the GMR sensor in a GMR-EC probe.

Let us consider one case where the image resulting from the two-dimensional scanning of a defect depicted the eddy-current density inside the metal. If that were possible the images obtained should be closely related to the defect geometry.

2.2 Using Constant Field Planar Probes

The pancake coils present excitation fields which are not invariant under translations, but those translations are inevitable when a given area is scanned. To obtain such invariant field a planar excitation coil was constructed with a zone of parallel conductors to produce an excitation field with spatially invariant under the scanning translations. Figure 3 depicts such probe. We used sinusoidal excitation at the frequency f_{ex}=1.0 kHz and amplitude I_{ex}=200 mA.
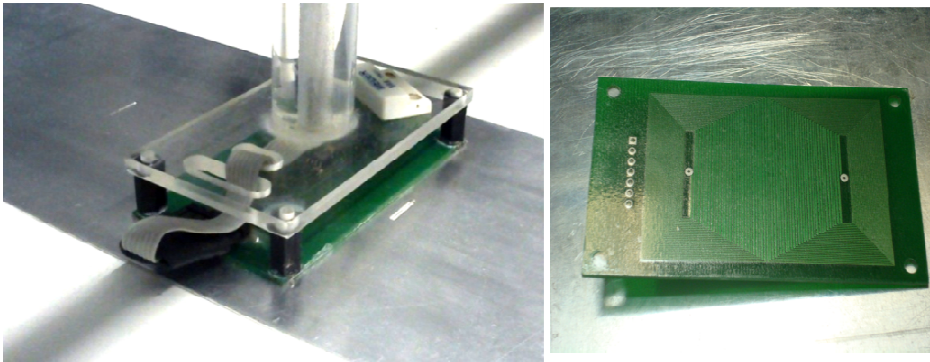
Figure 3. The planar probe used to obtain an invariant excitation field under the scanning translations.

A GMR sensor is provided on the upper side of the planar probe. The GMR sensitive axis is aligned with the excitation current in order not to sense the strong excitation field or the field originated by eddy currents in a homogeneous plane conductor, but responding to the eddies of current induced by the perturbations created by material defects.

2.3 The Induced Eddy Currents

The eddy currents generated inside the metal by induction are spatially uniform inside the restricted area under the probe, where the constant field is applied. The variation along the material thickness is compatible with the standard penetration depth, which depends on the conductivity and on the operation frequency. Thus, under the influence of the constant excitation field, and in a situation free of defects, the induction currents follow parallel lines oriented in the same direction of the excitation, but with a phase whose difference to opposition (π radians) depends on the material conductivity.

Figure 4 depicts the situation characterized by the presence of a defect. The current lines deviate from the defect, but may be decomposed into one uniform component and a perturbation. This perturbation may be represented as a collection of eddies of current.
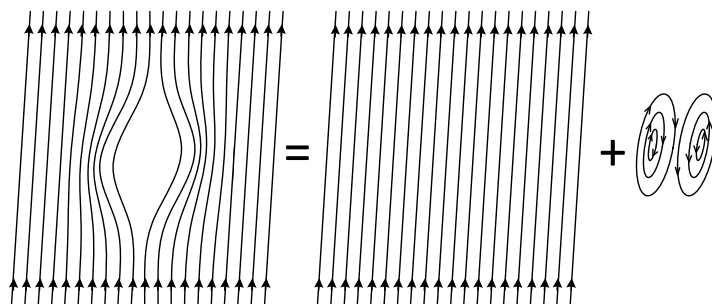

Figure 4. The inductive currents, in the presence of a defect, may be divided into a uniform part and perturbation eddies.

Being the magnetic field sensor insensitive to the uniform part of the currents, due to the orientation of the GMR sensitive axis parallel to the uniform current lines, the eddies of current become the most important current component for the defect detection. Let us represent such perturbation as a superposition of elemental current

dipoles. Let us consider a space discretization of the plane material surface, as represented in Fig.5, compatible with the real scanning step equal to 0.5 mm.

Note that this type of current discretization contains all information about the current, on the condition that the current dipolar intensity along the surface boundary elements vanishes.
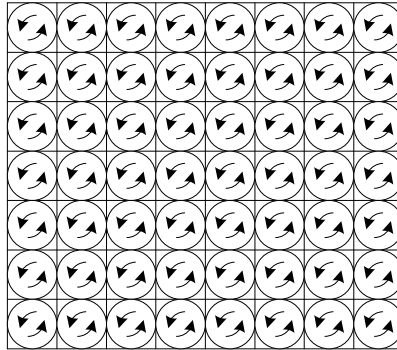

Figure 5. Surface space discretization. Each elemental square contains a current dipole.

The current perturbation may be represented in matrix form as $\mathbf{I}_p(i, j)$

$$\mathbf{I}_p(i, j) = \mathbf{A}(i, j)\, i_u \qquad (1)$$

where i_u is a unitary dipolar current, which may be materialized as a circular small loop with diameter equal to the space discretization and $\mathbf{A}(i, j)$ is the matrix representation of the complex amplitudes of the discrete dipolar currents. The approximation which results from the consideration of a spatial real configuration for an elemental dipolar current is very important, because the magnetic field to be measured will be represented as a linear combination of the unitary currents field.

3. Magnetic Field Measurement

The probe uses a single axis (y-axis) giant magneto-resistor sensor to measure one component of the magnetic field which is generated by the inductive currents. The sensor, produced by Non-Volatile Electronics[3], contains four magneto-resistors in a bridge configuration. Two magneto-resistors are shielded by permalloy high permeability pieces which also work as flux concentrators to enhance the sensitivity of the other two. Due to the V-shape characteristic of these sensors a tiny permanent magnet is used to establish the quiescent working point in the middle of a linear zone of the characteristic. The sensor sensitivity is equal to 40 mV/V mT, corresponding to 200 mV/mT if the bridge sensor is powered with a ±5 V power source. The sensor output is applied to an instrumentation amplifier with a voltage gain equal to 40 dB. The sensor voltage and the excitation current are acquired using a data acquisition system working at the sample frequency f_S=100 kHz. At each single point of a grid with a step equal to 0.5 mm in both directions, 100 periods of both signals are acquired and these data are used to determine the amplitudes of both signals and the phase difference between them. A sine-fitting algorithm based on a least square method is used, representing a good choice to minimize the effect of sensor nonlinearity, quantization error, or random noise.

Let us represent by $\mathbf{H}_y$ the matrix ofthe values obtained by the measurement of the field y-component on a given scanned area using the position system depicted in Fig. 6. One first inspection of the measured $\mathbf{H}_y$values must confirm that they vanish along the matrix boundary. If this is not the case, some other defect may be in range, as is usually the case of the material edges. Sometimes it may occur that the measured values along the boundary tend towards a constant value different from zero. This means that there is a misalignment of the field detector in relation to the imposed excitation currents, and some small fraction of the excitation field is detected. In this case the measured data must be corrected.
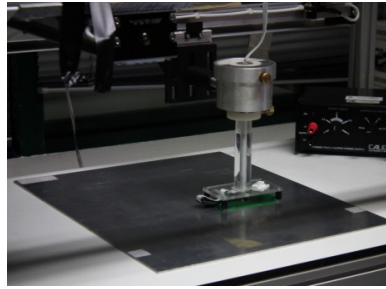
Figure 6. Scanning an aluminium plate where a linear defect was machined.

The measured field $\mathbf{H}_y$ may be represented as

$$\mathbf{H}_y(m,n) = \sum_{i,j} \mathbf{h}_y(m-i, n-j)\mathbf{A}(i,j) \tag{2}$$

where$\mathbf{h}_y$ represents the matrix of field values (y-component) that would be sensed on the (*m,n*) points when a unit dipolar current is positioned on (*i,j*). Equation (2) assumes the form of a convolution between the kernel $\mathbf{h}_y$ and the matrix of the amplitudes$\mathbf{A}$. Later in this paper we shall attempt the deconvolution of (2) to obtain the amplitudes from the measurements.

4. The Direct Problem

In the so called direct problem, when applied to the present case, one defect is considered and a preview of the measurements is obtained by some analytical or numerical process. Considering the two-dimensional problem of current flow around a linear crack with end points at $(-L, 0)$ and $(+L, 0)$ it is possible to use the following conformal mapping witch transforms the complex $Z = x + j\,y$ plane into the complex potential *P*[4]

$$P = A[Z\cos\alpha - j(Z^2 - L^2)^{1/2}\sin\alpha] \tag{3}$$

With the derivative of P we can obtain the components of a flux that can be interpreted as a current density:

$$J = J_x + j\,J_y = \overline{P'(Z)} = A\left[\cos\alpha \pm j\frac{Z\sin\alpha}{(Z^2 - L^2)^{1/2}}\right] \tag{4}$$

In (3) and (4)α is the anglebetween the crack and the current main flow and the upper bar represents complex conjugate. Figure 7 depicts the current flow around a crack for $\alpha = \pi/4$ and *L*=1 cm.
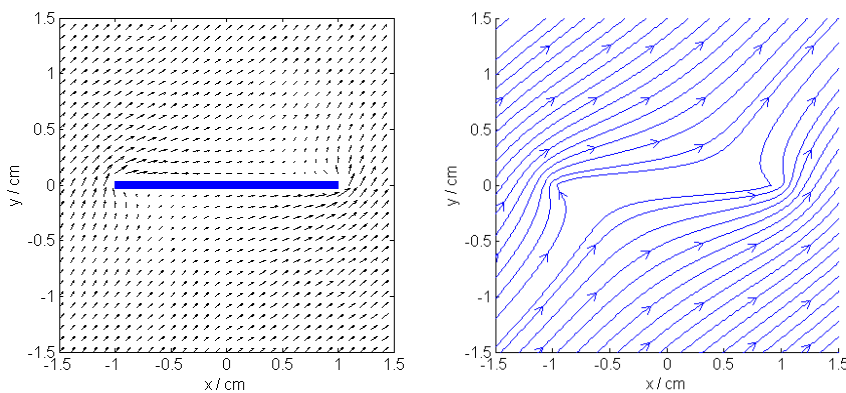

Figure 7. The current around a linear crack, depicted with arrows (left side) or with current lines (right side).

The current disturbances may be obtained if we subtract the constant density current (at 45º in the present case) from the current density depicted in Fig.7. The resulting current perturbation is represented in the Fig. 8 pictures.
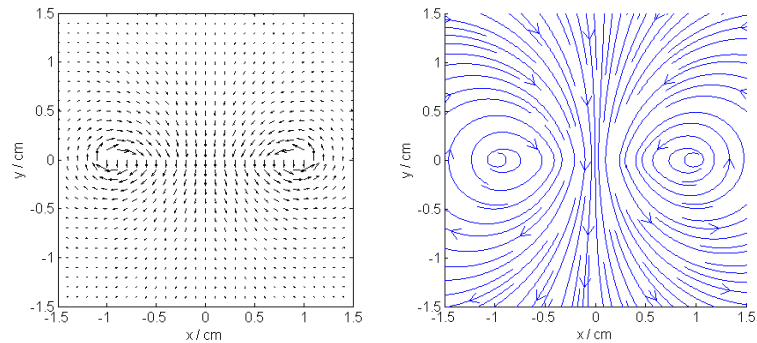

Figure 8. The perturbation of the current lines due to a linear crack, depicted as in Fig. 7.

As was referred previously, the field detector reads the field component parallel to the excitation current. When no defects are present, the induction currents although in phase opposition, follow parallel paths to the excitation as well. Thus, the detector doesn't sense any field in a situation without defects. In the presence of defects the perturbation eddies of current, like those represented in Fig. 8, generate a field that can be measured. The magnetic field produced by this current was calculated using the Biot-Savart law, and the y-component of the magnetic flux density is represented in Fig. 9.
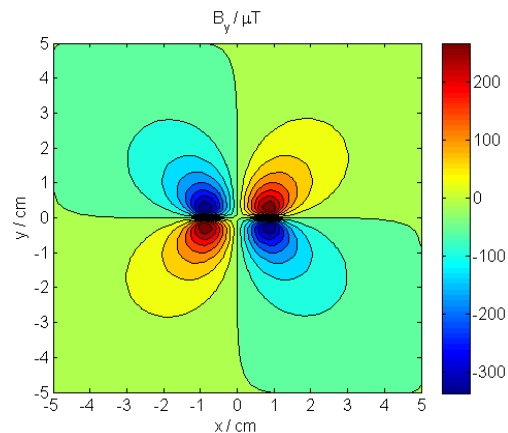

Figure 9. The B_y-component of the magnetic flux density calculated from the current perturbation depicted in Fig. 8.

The result obtained with simulation may be compared in an iterative process to estimate the characteristics of a real crack [4].

5. The Inverse Problem

As was stated before the geometrical characteristics of a defect may be obtained by an iterative solution of the direct problem. The defect geometry is iteratively changed in an attempt to minimize the difference between the measured and the calculated fields. In our case, we follow a different approach. We shall attempt the inversion of (2), reconstructing the array of the amplitudes **A**, from the measured field values $\mathbf{H}_y$ and assuming a convenient kernel $\mathbf{h}_y$.
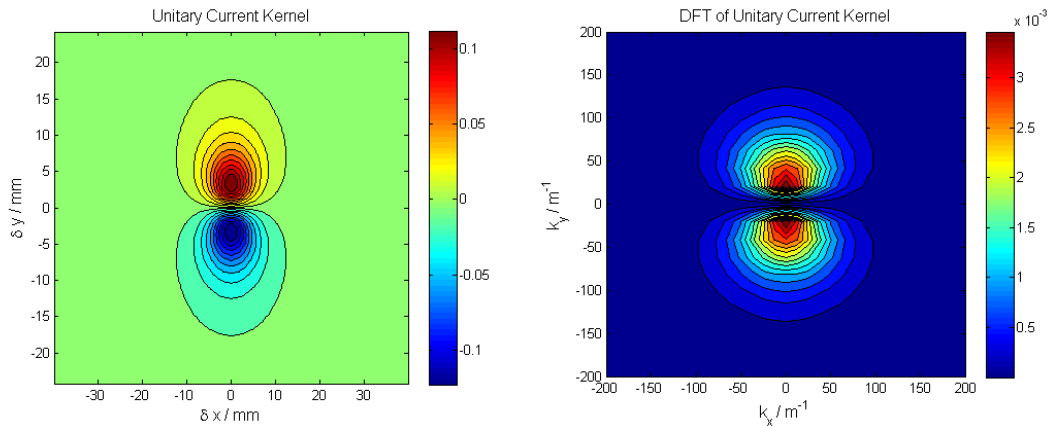
Figure 10. The unitary kernel$\mathbf{h}_y$ (left side) and itsdiscrete spatial Fourier transform $\hat{\mathbf{h}}_y$ (right side).

It is well known that the Fourier transform changes the convolution into a simple multiplication. Thus, it is recommended to use it here, in the discrete form. Thus (2) is transformed into

$$\hat{\mathbf{H}}_y = \hat{\mathbf{h}}_y \times \hat{\mathbf{A}} \tag{5}$$

where we represent the discrete Fourier transforms (DFT) with an hat.It is appropriate to remember that the three quantities in (5) are represented as matrices for pure convenience. Thus, the multiplication is performed element by element, being not a matrix multiplication. It is not possible to obtain $\hat{\mathbf{A}}$ dividing the measured data $\hat{\mathbf{H}}_y$ by the kernel $\hat{\mathbf{h}}_y$ because the data obtained by measurement always present some noise, and the kernel $\hat{\mathbf{h}}_y$ is very small for the highest wave numbers. Thus, from now on, we shall separate the measured data into a noiseless component $\hat{\mathbf{H}}_y^0$ and the noise $\hat{\boldsymbol{\eta}}$:

$$\hat{\mathbf{H}}_y = \hat{\mathbf{H}}_y^0 + \hat{\boldsymbol{\eta}} \tag{6}$$

The dipolar current density is now expressed as the sum of a current distribution that would be obtained if the acquired data were noiseless with the term that includes the effect of noise.

$$\hat{\mathbf{A}} = \frac{\hat{\mathbf{H}}_y^0}{\hat{\mathbf{h}}_y} + \frac{\hat{\boldsymbol{\eta}}}{\hat{\mathbf{h}}_y} = \hat{\mathbf{A}}^0 + \frac{\hat{\boldsymbol{\eta}}}{\hat{\mathbf{h}}_y} \tag{7}$$

We shall use Tikhonov regularization [7] to overcome the inversion difficulty. The kernel DFT is changed to

$$\hat{\mathbf{h}}_y^\mu = \frac{|\hat{\mathbf{h}}_y|^2 + \mu}{\hat{\mathbf{h}}_y^*} \quad , \quad \hat{\mathbf{h}}_y = \lim_{\mu \to 0} \hat{\mathbf{h}}_y^\mu \tag{8}$$

where $\mu > 0$ is the regularization parameter and * represents the complex conjugate. The choice of the optimum value of the regularization parameter was made, starting with large values of μ and checking smaller values until the resulting image begins to degrade. The inversion process may proceed by using the inverse DFT of the regularized dipolar current density:

$$\hat{\mathbf{A}}^\mu = \frac{\hat{\mathbf{H}}_y}{\hat{\mathbf{h}}_y^\mu} \tag{9}$$

Note that the equation (9) may be written in the form

$$\hat{\mathbf{A}}^{\mu} = \frac{\hat{\mathbf{h}}_y^*}{|\hat{\mathbf{h}}_y|^2 + \mu} \hat{\mathbf{H}}_y = \frac{|\hat{\mathbf{h}}_y|^2}{|\hat{\mathbf{h}}_y|^2 + \mu} \frac{\hat{\mathbf{H}}_y}{\hat{\mathbf{h}}_y} = \hat{\mathbf{W}}_\mu \frac{\hat{\mathbf{H}}_y}{\hat{\mathbf{h}}_y} \tag{10}$$

showing that the Tikhonov regularization[5] is equivalent to a low-pass filter $\hat{W}_\mu$ actuating in the frequency domain.The regularized dipolar amplitudes may be obtained using the inverse discrete Fourier transform

5.1 Choice of the Regularization Parameter

The Tikhonov regularization method is very fast. Thus, it is possible to solve repeatedly the inverse problem and represent graphically the results for parameter values within a range that is previously determined for a known class of problems. This process relies on the human observation. In the future some artificial intelligence algorithm will be tried to accomplish this function.

6. Results and Conclusions

Figure 11 represents the measured y-component of the magnetic field when the scanned area included a two centimeters long crack oriented perpendicularly to the imposed excitation current.
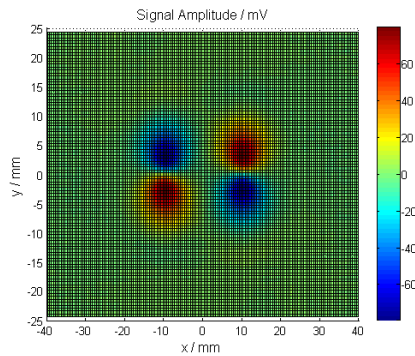

Figure 11. The data**H**$_y$.

These data were used to preview the dipolar current amplitudes **A** depicted in Fig. 12 using the kernel represented in Fig.10.
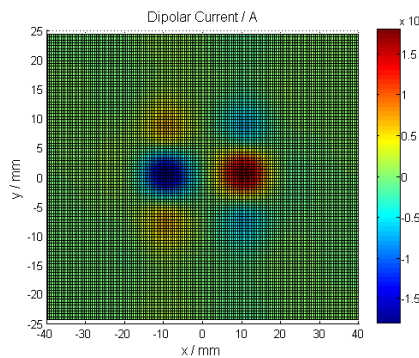

Figure 12. The dipolar current amplitudes **A**.

According to the color map in Fig. 12 the red color represents eddies of current circulating in the counterclockwise sense and the blue color represents eddies circulating in the opposite sense. The currents represented in Fig. 12 are the perturbations resulting from the presence of the crack. These currents are represented as arrows in Fig. 13 and totally reconstructed in Fig. 14.
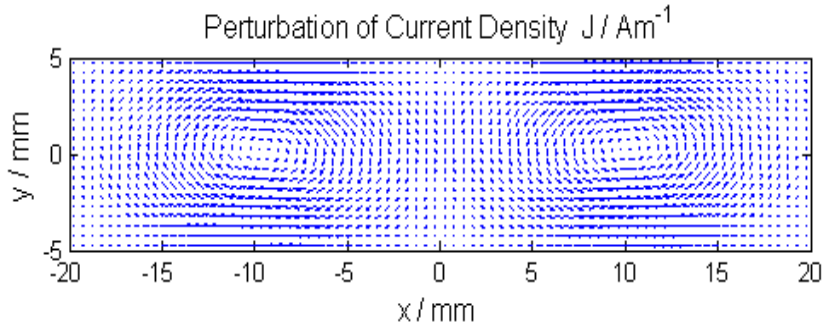
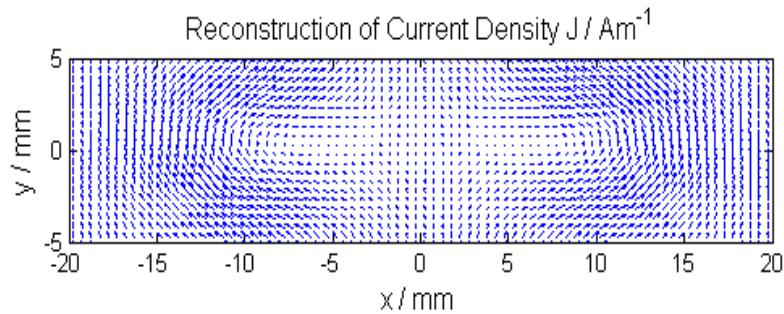**Figure 13.** The perturbation current eddies.

Figure 14. The totally reconstructed eddy current.

To identify the presence of defects it is also useful to depict the total current density in a colour graphic way. Inside the areas containingdefectsthe current density is minimal. Fig. 15 depicts the total current density previously calculated. The dark blue zone clearly shows the presence of the defect, and the red zones represent the current flowing around the crack.
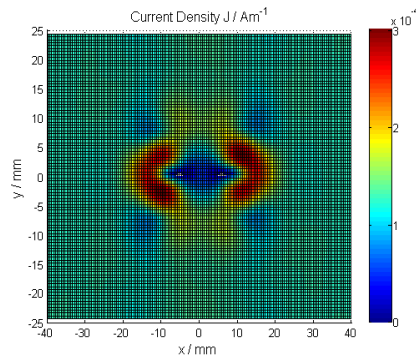
Figure 15. The totally reconstructed eddy current.

From the results presented in this section we may conclude that it is possible, in some circumstances, to obtain the maps describing in an image the eddy currents inside a conductive material under eddy current testing. These circumstances are related to the thickness of the current layers in plane conductors. If the standard depth of penetration is greater than the material thickness or much smaller his method performs adequately.

Acknowledgment

This work was developed under the Instituto de Telecomunicações projects KeMANDE and OMEGA and supported in part by the Portuguese Science and Technology Foundation (FCT) projects: PEst-OE/EEI/LA0008/2013, SFRH/BD/81856/2011 and SFRH/BD/81857/2011. This support is gratefully acknowledged.

References

1. Pasadas D., Rocha T., RamosH.G. andLopes Ribeiro A., Measurement 45 (2012), p393.
2. Ramos H.G., Kufrin L. and Ribeiro A.L., in Review of Progress in Quantitative Nondestructive Evaluation, (eds) Thompson D.O. and ChimentiD.E.,San Diego-USA (2010), p 673.
3. Non Volatile Electronics @http://www.nve.com.
4. Lopes Ribeiro A., Ramos H.G. andPostolache O., Measurement 45 (2012), p 213.
5. Bertero M. and Boccacci P., Introduction to Inverse Problems in Imaging, Institute of Physics Publishing (1998) p 107.